Modeling the Observed Controlled-Source Waveform Changes at Parkfiled

V. A. Korneev, T. V. McEvilly and E. D. Karageorgi

RESEARCH OBJECTIVES

A unique data set for the study of wave propagation in the San Andreas fault zone has been acquired in the Parkfield Prediction Experiment (PPE) underway in central California). Data have been collected with a ten-station borehole network in a search for evidence of changes associated with the nucleation process of the anticipated M6 earthquake at Parkfield. More than 6000 earthquakes have been recorded since 1987 in the magnitude range -1<M<5. In addition, seismograms for 720 source-receiver paths have been obtained for repeated illumination of the network using a large shear-wave Vibroseis, from June 1987 until November, 1996, when the program ended. That investigation reported significant travel-time changes in the coda of S for paths crossing the fault zone southeast from the epicenter of the 1966 M6 earthquake. Progressively decreasing travel times in the anomalous region reached 50 msec or more by the end of the study. Changes in frequency content and polarization were also found and those effects, too, could be localized to the zone of common nucleation and rupture onset for the previous M6 earthquakes, and, possibly, the region of slip initiation for the great earthquake of 1857). The temporal pattern in these variations appears to be synchronous with changes in deformation and seismicity measured independently. Because similar variations are not seen in the waveforms recorded from microearthquakes in the same part of the fault, in previous studies we conclude that changing fluid conditions in the uppermost section of the fault zone in response to deeper, tectonic stress perturbations are the likely cause of the temporal variations. Exploring that possibility further for plausible velocity perturbations in the shallow fault zone, in this study we model the observed waveform changes numerically.

APPROACH

At Parkfield the San Andreas fault zone is a striking near-vertical low-velocity zone , and it very clearly acts as a waveguide for seismic energy from earthquakes on the fault and from surface sources . Velocity models there show high Vp/Vs ratio along the fault near the surface and at depth within the fault zone, and a pronounced vertical velocity gradient in the upper 2 km of the section. The geometry of the Vibroseis source and receiver network, the approximate two-dimensionality of the fault zone in the region of the travel-time anomaly, and the existence of detailed P- and S-wave velocity models for the area all combine to provide well-determined constraints in modeling the observations. In this study we consider only data recorded at stations VCA and JCN from vibrator site VP2. At VP2 we have the routine Vibroseis monitoring data from the repeated point source, as well as a cross array of sources with 17 VPs on each leg. We confined our modeling exercise to the VP2 data for VCA and JCN for several reasons. Both source-receiver paths are in the anomalous region and reveal substantial travel-time variations. The two paths are approximately co-linear and orthogonal to the San Andreas fault, permitting the use of a two-dimensional formulation in simulating wave propagation. The paths sample segments of similar-length on the two sides of the fault zone. Finally, the data profile from the closely-spaced source array at VP2 defines the spatial coherency of the wavefield that is helpful in phase identification and interpretation of the recorded wavefield. The velocity model used in numerical simulation incorporates the known properties of the region, where tomographic three-dimensional velocity models have already been determined . A major factor controlling the character of wave propagation at short range from a surface source is the severity of the shallow vertical velocity gradient. We found a velocity gradient model by matching the observed and computed direct arrivals in the early part of seismograms. For the NE side of the fault, the direct arrivals at JCN could be matched with a velocity profile reduced to 0.76 of that for VCA, and to 0.5 for the narrow fault zone, modeled as a vertical layer with a thickness of 200 meters, bounded by interfaces F1 and F2 . Computations were performed using a two-dimensional elastic finite-difference formulation with a staggered grid. The model was digitized on a 2200 x 500 grid with 5m spacing, which yields a model space of 11 km horizontal and 2.5 km vertical extent, as depicted in the figure.

RESULTS

A snapshot of elastic field development is presented in Figure 1. Two features dominate the process: energy trapping near the surface by the shallow gradient, and wavefield scattering from the fault zone. Most of the energy is confined to the upper part of the section in multiple reflections at the free surface, producing a complex train of surface-guided waves made up of many arriving phases.

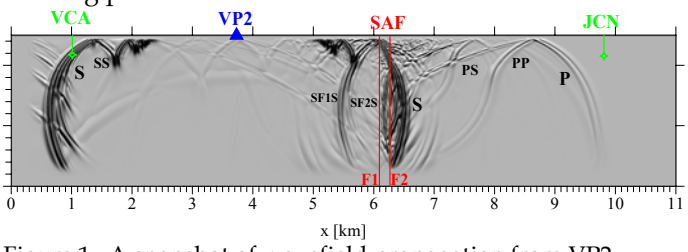

Figure 1. A snapshot of wavefield propagation from VP2 source at 2 seconds

Synthetic seismograms (horizontal component) are shown in Figure 2 . Initial direct P and S waves arrive

around 1 sec and 2 sec at VCA. At JCN they are seen at 2.2 sec and 4.4 sec. Because the receivers are located at depth, both up- and down-going energy is seen, as well as horizontally propagating turning-point waves.

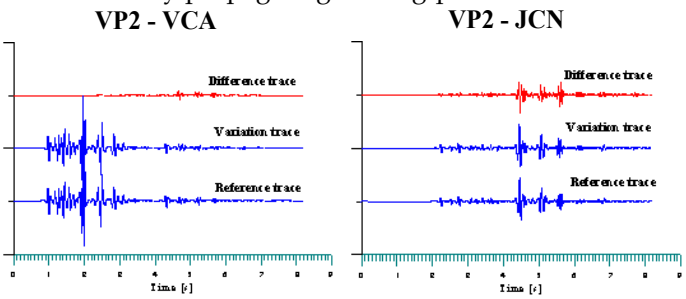

Figure 2. Synthetic traces for variation modeling.

The signature of the fault zone and shallow gradient on the wavefield is dramatic. In the interval between the first-arriving P and S waves at VCA are the surface-generated multiples and conversions. The latter are especially strong for P-waves, e.g., PS, PPS, etc. Strong reflections are also produced by the fault-zone boundaries, F1 and F2 . PF_1P, the first F1 reflection at VCA, is small and masked by the large direct S wave just before it. F2 reflections at VCA have passed twice through the fault zone, and these late phases such as PF_2PP (3.5s) and SF_2S (4.7s) are quite strong, arriving well after the direct waves have passed . At JCN the internal fault-zone reflections produce sequences of strong, distinct arrivals following the direct P and S waves. The times in the synthetic seismograms where large travel-time changes were observed in the monitoring project at VCA and JCN contain significant energy that has been scattered from the fault zone. This result suggests a ready explanation for the cause of the observed progressively decreasing travel-times . For the path VP2-VCA the changes were seen at arrival times after 3.5 seconds, i.e., for our model seismograms, after the direct waves have passed and the fault-zone reflected waves are arriving. On the other hand, the travel-time changes for the VP2-JCN fault-crossing path begin with the arrival of the direct P wave and occur through the entire seismogram. We take these results to be strong evidence that the observed variations are most likely caused by changes within the fault zone itself. To test the fault-zone hypothesis we modeled travel-time variations that would be produced by a small velocity change at the fault. To compare with seismograms for the reference model described above, we computed new seismograms at VCA and JCN for a velocity increase of 6% localized in the narrow fault zone. These seismograms are shown in Figure 2 along with their differences from the reference traces. As expected, the changes at VCA appear only after the fault-zone F2 reflections reach the station, while at JCN the travel-time advance begins with the initial P wave and increases throughout the seismogram. The magnitude of the calculated travel-time variations match the observed data quite closely. In Figure 3 we make a direct comparison with the Vibroseis data, where the synthetic-derived variations are plotted with the observed travel-time shifts at both stations. The match is quite good in character, magnitude and timing. The first unstable wavelet at VCA corresponds well to the PF_2PP reflection from the fault zone. At JCN the pattern of steady increase in the travel-time shift due to progressive involvement of slower S waves is quite clear.

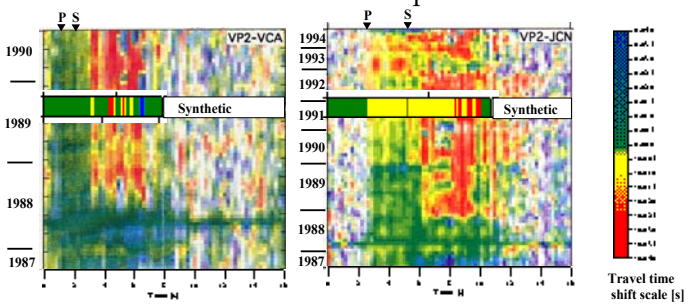

Figure 3. Comparizon of the observed and modeled variations.

SIGNIFICANCE OF FINDINGS

Previous studies clearly detected real changes in travel-times in the 8-year controlled-source monitoring program at Parkfield, and localized the anomalous changes to a region southeastward from Middle Mountain, roughly in the presumed nucleation zone for the past and future M6 Parkfield earthquakes. Their best hypothesis for the phenomenon called for changing fluid conditions in the shallow section above the fault zone. Our study supports that hypothesis and offers a more quantitative model for the actual wave propagation involved. The final link in the puzzle lies in the responsible mechanism for the velocity change in the fault zone. We are inclined to accept the idea of a deeper tectonic deformation that somehow changes the fluid environment in the shallow fault zone. The striking importance of the shallow vertical velocity gradient cannot be overstated. It is clear from this study that surface sources employed in highly heterogeneous environments such as the San Andreas fault zone can be expected to generate an overwhelming near-surface wave field that must be dealt with in looking for deeper images. If the individual phases can be identified, however, they may provide an important tool for studying near-surface details of the fault structure.

PUBLICATIONS

V. A. Korneev, T. V. McEvilly and E. D. Karageorgi, 1999, Seismological studies at Parkfield VIII: Modeling the Observed Controlled-Source Wave Changes at Parkfield,, Submitted to Bull. Seism. Soc. of Am.

FUNDING

Data processing was done at the Center for Computational Seismology (CCS) at LBNL, which is operated by the University of California for the U.S. Department of Energy

(DOE) under contract No. DE-AC03-76SF00098. The USGS provided financial support for this research through NEHRP award 1434-95-G-2540.